

Superconducting specific heat jump $\Delta C_{\text{el}} \propto T_c^\beta$ ($\beta \approx 2$) for $\text{K}_{1-x}\text{Na}_x\text{Fe}_2\text{As}_2$

V. Grinenko,^{1,*} D.V. Efremov,¹ S.-L. Drechsler,^{1,†} S. Aswartham,¹ D. Gruner,¹ M. Roslova,^{1,2}
I. Morozov,^{1,2} K. Nenkov,¹ S. Wurmehl,^{1,3} A.U.B. Wolter,¹ B. Holzapfel,^{1,4} and B. Büchner^{1,3}

¹Leibniz-Institute for Solid State and Materials Research, IFW-Dresden, D-01171 Dresden, Germany

²Lomonosov Moscow State University, GSP-1, Leninskie Gory, Moscow, 119991, Russian Federation

³Institut für Festkörperphysik, TU Dresden, D-01062 Dresden, Germany

⁴Karlsruhe Institute of Technology (KIT), Hermann-von-Helmholtz-Platz 1, 76344 Eggenstein-Leopoldshafen, Germany

(Dated: August 7, 2018)

We present a systematic study of the electronic specific heat jump (ΔC_{el}) at the superconducting transition temperature T_c of $\text{K}_{1-x}\text{Na}_x\text{Fe}_2\text{As}_2$. Both T_c and ΔC_{el} monotonously decrease with increasing x . The specific heat jump scales approximately with a power-law, $\Delta C_{\text{el}} \propto T_c^\beta$, with $\beta \approx 2$ determined by the impurity scattering rate, in contrast to most iron-pnictide superconductors, where the remarkable Bud'ko-Ni-Canfield (BNC) scaling $\Delta C_{\text{el}} \propto T_c^3$ has been found. Both the T dependence of $C_{\text{el}}(T)$ in the superconducting state and the nearly quadratic scaling of ΔC_{el} at T_c are well described by the Eliashberg-theory for a two-band d -wave superconductor with weak pair-breaking due to nonmagnetic impurities. The disorder induced by the Na substitution significantly suppresses the small gaps leading to gapless states in the slightly disordered superconductor, which results in a large observed residual Sommerfeld coefficient in the superconducting state for $x > 0$.

PACS numbers: 74.25.Bt, 74.25.Dw, 74.25.Jb, 65.40.Ba

The overwhelming majority of iron-pnictide superconductors exhibit several puzzling universal features. One of them is the Bud'ko-Ni-Canfield (BNC) scaling of the specific heat (SH) jump (ΔC_{el}) at the superconducting transition temperature (T_c) [1]. For example, $\text{Ba}(\text{Fe}_{1-x}\text{Co}_x)_2\text{As}_2$, $\text{Ba}(\text{Fe}_{1-x}\text{Ni}_x)_2\text{As}_2$, and many other compounds [1–3] show a $\Delta C_{\text{el}} \propto T_c^3$ behavior. Several scenarios were proposed to explain this unusual behavior [2, 4–6] or at least deviations from the BCS-theory prediction were ascribed to the interplay of coexisting spin density wave (SDW) state and superconductivity (SC) [7, 8]. One of the possible reasons for the $\Delta C_{\text{el}} \propto T_c^3$ behavior might be a strong pair-breaking, which is an intrinsic property of many Fe pnictide superconductors [2, 4] due to the vicinity of competing magnetic (spin-density-wave) phases and/or the always present impurities. Another approach to explain the cubic BNC scaling rests on the assumption of a non-Fermi liquid behavior near a magnetic critical point. In such a special situation a $T_c^3(T_c^2)$ scaling in three (and two) dimensions, respectively, based on sophisticated field-theory arguments was suggested by J. Zaanen [5, 9]. Also, the possible influence of thermal SDW fluctuations on the SH jump value was emphasized in Ref. 6. Recently, it was found that the „universal” cubic BNC scaling fails for the heavily hole-doped $\text{K}_x\text{Ba}_{1-x}\text{Fe}_2\text{As}_2$ at a K doping $x > 0.7$ [10]. The authors suggested that the observed deviations point to significant changes in the nature of the superconducting state. For example, in stoichiometric KFe_2As_2 d -wave [11–13] or s -wave SC with accidental nodes [14–16] were suggested by different experiments. From the theoretical side it was predicted that with increasing hole-doping the superconducting order parameter changes from nodeless s_\pm at the optimal doping to a nodal s_\pm [17] or d -wave

state [18] in KFe_2As_2 via possible intermediate $s + is$ or $s + id$ -wave states [19], respectively. In this paper we show that among the Fe pnictides at least two different groups can be distinguished by their ΔC_{el} vs. T_c plot. The first group [1, 10] is related to the majority of Fe pnictides as proposed previously. $\text{K}_{1-x}\text{Na}_x\text{Fe}_2\text{As}_2$ belongs to the second group which scales almost conventionally with $\Delta C_{\text{el}} \propto T_c^2$. Both the observed ΔC_{el} vs. T_c behavior and the T dependence of C_{el} are consistent with multiband d -wave SC in $\text{K}_{1-x}\text{Na}_x\text{Fe}_2\text{As}_2$.

$\text{K}_{1-x}\text{Na}_x\text{Fe}_2\text{As}_2$ single crystals with a typical mass of about 1-2 mg and several mm in-plane dimensions were grown by the self-flux method. The compositions and the phase purity of the investigated samples were determined by an EDX analysis in a scanning electron microscope, and by x-ray analysis [20]. The SH data were obtained by a relaxation technique in a Physical Property Measurement System (PPMS), Quantum Design. The resistivity was measured by the standard four-contact method in the PPMS. The magnetic dc susceptibility as a function of temperature was measured using a commercial SQUID magnetometer, Quantum Design.

The T dependencies of the volume susceptibility χ_v of $\text{K}_{1-x}\text{Na}_x\text{Fe}_2\text{As}_2$ for different x values are shown in Fig. 1a. All investigated samples have a large superconducting volume fraction. The T dependencies of the molar susceptibility χ_m of $\text{K}_{1-x}\text{Na}_x\text{Fe}_2\text{As}_2$ for different x values measured for $H \parallel ab = 10\text{ kOe}$ are shown in Fig. 1b. The χ_m in the normal state is nearly independent on the temperature for $50\text{ K} \leq T \leq 150\text{ K}$. This behavior is expected for the paramagnetic Pauli susceptibility of a Fermi liquid. The upturn below $T = 50\text{ K}$ indicates a small amount of magnetic impurities [21]. The measured χ_m values are considerably lower than the data

reported previously in Ref. 22 for KFe_2As_2 with a cluster glass behavior and similar to the Pauli susceptibility value reported in Ref. 21, where an impurity contribution had already been subtracted. The magnetization curves measured at $T = 5\text{K}$ (see the inset in Fig. 1b) slightly deviate from a linear dependence. This allows us to estimate the concentration of magnetic impurities n in the samples assuming that it is related to paramagnetic Fe atoms. In this case, we arrived at $n \lesssim 0.1\text{ mol}\%$ for all investigated samples [20]. The low value of n suggests that the Na substitution does not induce local magnetic moments and that it can be considered as a nonmagnetic impurity. The corresponding linear static susceptibility at low temperatures after subtraction of the impurity contribution $\chi_s \approx 1.8(3) \cdot 10^{-3}\text{ cm}^3/\text{mol}$ is independent of the Na concentration within the error bars of the sample masses.

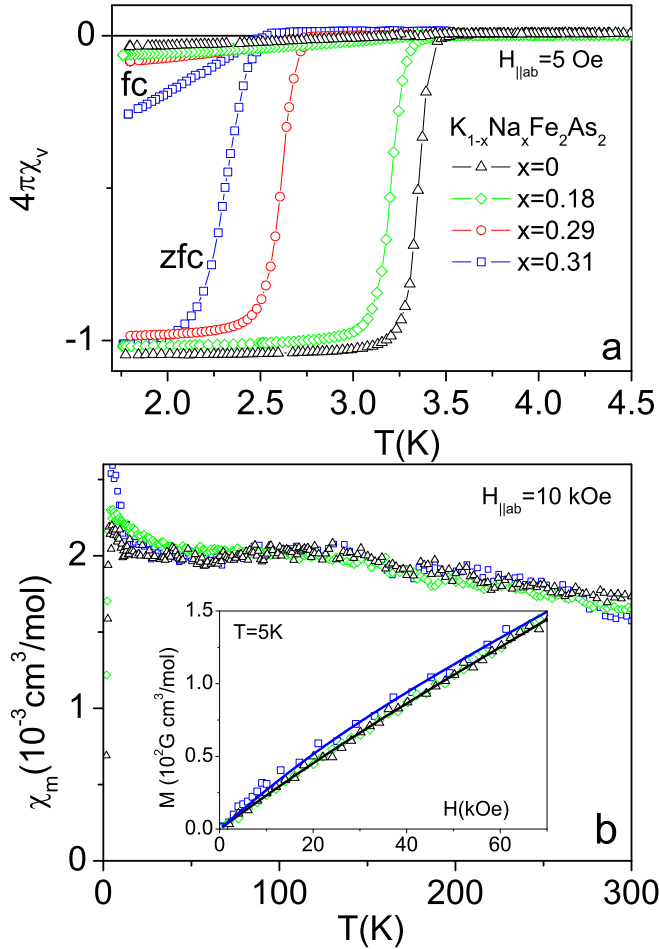


FIG. 1: (Color online) (a) Temperature dependence of the volume susceptibility χ_v measured in a magnetic field of $H \parallel ab = 5\text{ Oe}$. (b) Temperature dependence of the molar susceptibility χ_m measured in a magnetic field of $H \parallel ab = 10\text{ kOe}$. Inset: magnetization curves measured in an external field $H \parallel ab$. For explanation of the fitting curves see [20].

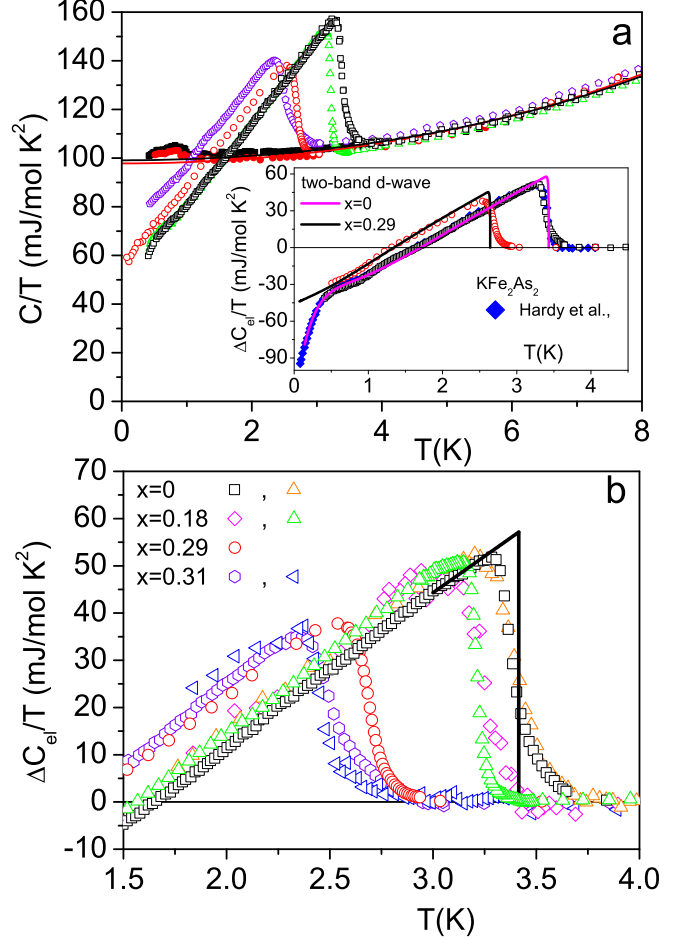


FIG. 2: (Color online) (a) Total specific heat C/T of $\text{K}_{1-x}\text{Na}_x\text{Fe}_2\text{As}_2$ vs. T . Open symbols: zero field data, closed symbols: data in an applied magnetic field $H \parallel c = 15\text{ kOe}$, solid lines: the fit of the normal-state specific heat (see text). The experimental data for $x=0.29$ at $T < 0.4\text{ K}$ are taken from Ref. 12. Inset: the specific heat $\Delta C_{\text{el}}/T = [C(0) - C(H)]/T$ vs. T for a sample with $x=0$ and 0.29 . Dots: experimental data; filled rhombus: data from Ref. [16] shown for comparison; solid line: calculation within two-band Eliashberg-theory for d -wave superconductors with nonmagnetic impurities and $T_{c0} = 3.44\text{ K}$ for the adopted clean limit. (b) $\Delta C_{\text{el}}/T$ near T_c for different samples of $\text{K}_{1-x}\text{Na}_x\text{Fe}_2\text{As}_2$. Solid lines are plotted according to the entropy equal-area construction method for determining T_c and $\Delta C_{\text{el}}/T_c$.

The SH $C(T)$ of $\text{K}_{1-x}\text{Na}_x\text{Fe}_2\text{As}_2$ is shown in Fig. 2. A clear superconducting anomaly is observed for all x in line with the susceptibility measurements. The normal state SH below $T = 10\text{ K}$ can be fitted by using the standard expression $C(T) = \gamma_n T + \beta T^3 + \eta T^5$, where γ_n is the normal-state Sommerfeld coefficient and the next two terms with β and η describe the lattice contribution to the SH. A value of $\gamma_n \approx 100\text{ mJ/mol K}^2$ was found for all investigated samples irrespective of the Na substitution within the error bars of the sample masses [20]. This

value is in accord with other published data for KFe_2As_2 [21, 23–26]. Inspecting Fig. 2a we see that the SH in the applied field of $H \parallel c = 15$ kOe deviates from a standard fit at $T \lesssim 1.5$ K forming a small hump, where the upper critical field obeys $H_{c2}^{\parallel c}(0) \lesssim 15$ kOe for $\text{K}_{1-x}\text{Na}_x\text{Fe}_2\text{As}_2$ according to Refs. 12, 16, 25, 27. The complete suppression of the SC by $H \parallel c = 15$ kOe is also supported by the resistivity measurements [20]. Thus, this hump cannot be ascribed to SC. A low- T anomaly related to magnetic impurities has been reported recently for KFe_2As_2 in Ref. 23. In our case the entropy confined in this anomaly is about 0.05% of $R \ln 2$ which is comparable to the value estimated in Ref. 23. By analogy, the hump can be related to a small amount of magnetic impurities observed in our samples in the magnetization measurements in Fig. 1. However, we cannot exclude intrinsic origins of this hump. We note that the low- T upturn in the normal state was also observed recently in KFe_2As_2 single crystals in the literature [16, 21, 27]. Therefore, further investigations are needed to clarify the nature of this anomalous behavior at low T . Above $T \sim 1.5$ K the electronic SH contains a dominant linear-in- T term as expected in the case of a clean Fermi liquid. Near T_c the corresponding Wilson ratio $R_W = \pi^2 k_B^2 \chi / (3\mu_B^2 \gamma_n) \sim 1$ for all investigated samples. This together with the doping independent Sommerfeld coefficient indicates that neither the density of states nor the strength of correlation effects are affected by the Na substitution.

The SH contribution related to the SC $\Delta C_{\text{el}}(T)/T = [C(0, T) - C(H, T)]/T$ is shown in Fig. 2a (inset) and in Fig. 2b, where $C(0, T)$ is the SH in zero magnetic field and $C(H, T)$ is the one measured in a magnetic field $H > H_{c2}$. The latter is taken to be the SH of the normal state. It is seen in Fig. 2b that the SH jump $\Delta C_{\text{el}}/T_c$ at T_c is a monotonic function of T_c . The ΔC_{el} data of our $\text{K}_{1-x}\text{Na}_x\text{Fe}_2\text{As}_2$ single crystals, and those taken from the literature for KFe_2As_2 samples with various T_c , together with many other Fe-arsenides and also some Fe-phosphides [3, 13, 28–30] are summarized in Fig. 3a. Two classes can be identified in the ΔC_{el} vs. T_c plot: The largest group with $\Delta C_{\text{el}} \propto T_c^3$, first reported in Ref. 1, 3, includes the overwhelming majority of Fe pnictides. Most of the superconductors in this region are believed to exhibit an s_{\pm} order parameter. Noteworthy, stoichiometric LiFeAs [31–33], which has a relatively low residual resistivity value $\rho_0 \sim 1.3 \mu\Omega\text{-cm}$ [34] as compared to most of the other Fe-based superconductors, and the impure Cu doped derivative [31], also fit to the BNC scaling, perfectly. A clearly distinct second class, we report here, consists of the $(\text{K}, \text{Na})\text{Fe}_2\text{As}_2$ systems. Phenomenologically this group scales approximately as T_c^β with an exponent $\beta \approx 2$ [35, 36] and can be associated with the pair-breaking dependence of ΔC_{el} in KFe_2As_2 due to disorder appearing during the sample synthesis of the stoichiometric compound or induced by the Na substitution. The sister compounds RbFe_2As_2 [37] and CsFe_2As_2 [38]

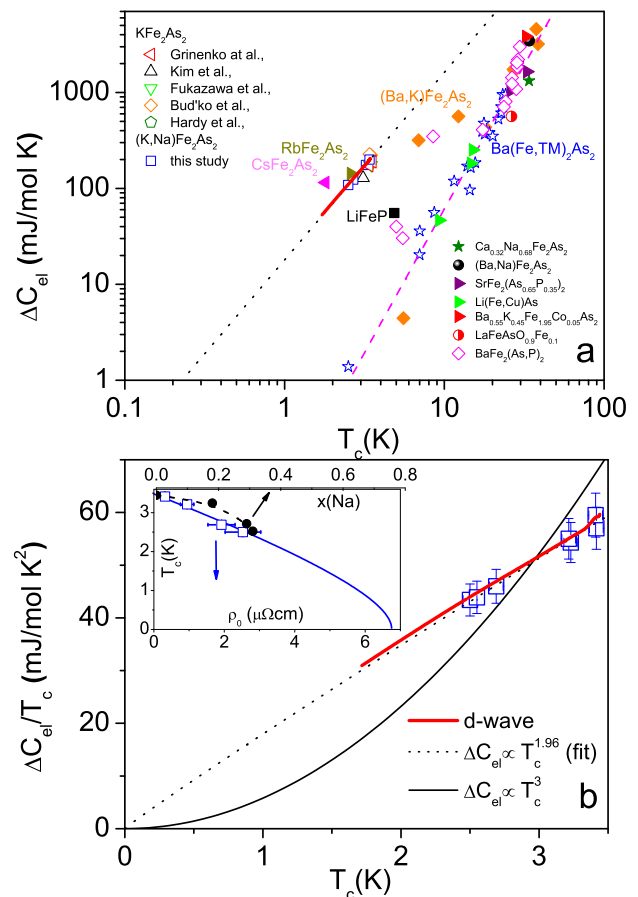


FIG. 3: (Color online) (a) The dependence of ΔC_{el} vs. T_c for different iron-pnictide superconductors. Solid curve: obtained within Eliashberg theory, dotted curve: the best fit of our experimental data by $\Delta C_{\text{el}} \propto T_c^\beta$ and dashed curve: BNC scaling $\Delta C_{\text{el}} \propto T_c^3$ [1, 10]. The data are taken from Refs. 21–24, 26 for KFe_2As_2 , CsFe_2As_2 [38], RbFe_2As_2 [37], $(\text{Ba}, \text{K})\text{Fe}_2\text{As}_2$ and $\text{Ba}(\text{Fe}, \text{TM})_2\text{As}_2$ [10] (TM - transition metal), LiFeP [28], $\text{Ca}_{0.32}\text{Na}_{0.68}\text{Fe}_2\text{As}_2$ [44], $(\text{Ba}, \text{Na})\text{Fe}_2\text{As}_2$ [45], $\text{SrFe}_2(\text{As}_{0.65}\text{P}_{0.35})_2$ [46], $\text{Li}(\text{Fe}, \text{Cu})\text{As}$ [31, 32], $\text{Ba}_{0.55}\text{K}_{0.45}\text{Fe}_{1.95}\text{Co}_{0.05}\text{As}_2$ [47], $\text{LaFeAsO}_{0.9}\text{Fe}_{0.1}$ [20, 48], $\text{BaFe}_2(\text{As}_{0.7}\text{P}_{0.3})_2$ [29]. (b) $\Delta C_{\text{el}}/T_c$ vs. T_c for $(\text{K}, \text{Na})\text{Fe}_2\text{As}_2$. Inset: T_c vs. residual resistivity ρ_0 and the Na substitution level x . Solid line: fit using the Abrikosov-Gor’kov formula [20], and the dashed curve: guide to the eye.

exhibit similar values of the SH jump and of T_c . However, further experimental studies on samples with a different amount of disorder are necessary to determine whether these systems behave similarly to KFe_2As_2 . Finally, several systems do not fit to any of these two classes: among them are $\text{Ba}_{1-x}\text{K}_x\text{Fe}_2\text{As}_2$ [10] with $0.7 < x < 1$, LiFeP [28], and $\text{BaFe}_2(\text{As}_{1-x}\text{P}_x)_2$ for $x \approx 0.2$ and 0.65 [30]. (Note that for $0.3 \lesssim x \lesssim 0.4$, in the vicinity of a critical point, a $T_c^{6.5 \pm 0.7}$ behavior has been suggested in Ref. 30, although the deviations from the BNC scaling is hardly visible on the logarithmic scale of Fig. 3a).

An inspection of Fig. 2a shows that the $C(T)/T$ for

$x = 0.29$ and 0.31 is nearly linear below T_c . For $x = 0$ the experimental data show a downturn at low T which can be explained by the presence of a small superconducting gap/gaps. Similar conclusions were drawn by the authors of Ref. 16, 21, 27. This low- T superconducting anomaly was not observed down to 0.1K for $x = 0.29$. The downturn is also absent in those KFe_2As_2 single crystals showing disorder related magnetic contributions, [12, 22] with only slightly reduced T_c . The enhancement of the impurity scattering with Na substitution is evidenced by the significant increase of the residual resistivity ρ_0 from $0.32(6) \mu\Omega\cdot\text{cm}$ at $x=0$ to $2.5(5) \mu\Omega\cdot\text{cm}$ at $x=0.31$, where the $\text{RRR}=\rho(300\text{K})/\rho_0$ value strongly decreases almost by an order of magnitude, from 1080 to 150 [20]. Therefore, by analogy with CeCoIn_5 [39] the observed unusual behavior of the SH might be ascribed to gapless SC in those bands with small superconducting gaps ($\sim \Delta_2$) which is further suppressed by the disorder induced pair-breaking. (Note, that non-magnetic impurities also suppress SC in the case of s_{\pm} order parameter [40].) In this case the Sommerfeld coefficient (γ_2) at low T for the Fermi surface sheets (FSS) with Δ_2 approaches almost the normal-state value, whereas the $\gamma_1(T)$ corresponding to the other FSS with the large gap Δ_1 shows the behavior expected for a single-band superconductor but with a formally large residual SH value $\gamma_2 \sim \gamma_r \gtrsim 50 \text{ mJ/mol-K}^2$ [41]. In particular, the temperature dependence of $\gamma_1(T) \sim \Delta C_{\text{el}}(T)/T \propto T$ at low T for samples with a part of the quasiparticles in a gapless state evidences the line nodes on the dominant order parameter with Δ_1 [12]. However, for the general description of the SH in clean and dirty samples, strictly speaking, a detailed investigation of a four-band model with a significant number of new parameters would be requested. But we believe that for the present level of understanding, the study of a less-complex effective two-band model as a minimum model is necessary.

The experimental data of the T dependence of the SH (inset of Fig. 2a) and the SH jump at T_c shown in Fig. 3 at all x can be reasonably well described by the two-band Eliashberg theory or a fully nodal $d_{x^2-y^2}$ -wave (in the notations of the folded Brillouin zone with 2 Fe per unit cell) superconductor with a weak pair-breaking included, but also with two rather differently coupled two groups of quasi-particles, therefore having rather different gap values. This situation is different from the standard s_{\pm} case considered, e.g. in the optimally-doped $(\text{Ba,K})\text{Fe}_2\text{As}_2$ [42] where usually at least *two* strongly interacting bands dominate the interband-coupling-driven SC within a higher-order multiband model, also including further weakly coupled bands. Note that other symmetries of the superconducting order parameter, such as s_{\pm} with accidental nodes and d_{xy} -wave have been proposed in the literature for KFe_2As_2 based on the low- T SH data [16, 27]. However, the discussion of these alternative scenarios is beyond the scope of the present paper.

For the calculations in the frame of the Eliashberg theory we used the same spin-fluctuation spectra as in Ref. 12 peaked at $\approx 8 \text{ meV}$ and an Einstein phonon peaked at 20meV , with the phenomenologically fitted coupling constants in two d -wave channels: $\lambda_{d1} = 0.818$, $\lambda_{d2} = 0.05$, $\lambda_{d12} = \lambda_{d21}N_2/N_1 = 0.13$ and also a weak uniform electron-phonon coupling $\lambda_{s1} = 0.1$, $\lambda_{s2} = 0.1$, $\lambda_{s12} = \lambda_{s21}N_2/N_1 = 0.04$, with the partial density of states of the effective two-band system obeying $N_2/N_1 = 2$. The nonmagnetic impurity scattering caused by the smaller, isovalent Na^+ ions has been treated in the adopted Born approximation [43]. For the calculations we adopted $\Gamma_2/\Gamma_1=5$, where Γ_1 and Γ_2 are the impurity scattering rates in band 1 and 2, correspondingly. Qualitatively, the Na position out of the FeAs-block position might be the reason for the different Γ values. Therefore, a stronger scattering effect for the Fe $3d_{xz}$ and $3d_{yz}$ orbitals oriented out of the Fe-plane as compared to the Fe $3d_{xy}$ orbitals might be expected. The value of the critical temperature in the clean limit adopted for the calculations is $T_{c0}=3.44\text{K}$. Note that the T_c suppression approximately follows the Abrikosov-Gor'kov pair-breaking theory with $\Gamma_{\text{eff}} \propto \rho_0$ (see the inset in Fig. 3b and Ref.20). Thus, adopting the Born approximation, we obtain a quantitative phenomenological description of our data shown in Figs. 2 and 3 within an effective two-band Eliashberg theory for a nodal d -wave superconductor.

In summary, we have shown that the Fe pnictide superconductors can be divided at least into two groups according to their ΔC_{el} vs. T_c plots. The main group contains the overwhelming majority of Fe pnictides. The second group consist of the heavily hole-doped superconductors $(\text{K,Na})\text{Fe}_2\text{As}_2$ and stands out from the other Fe pnictides with respect to its absolute values and its distinct scaling: $\Delta C_{\text{el}} \propto T_c^{\beta}$ with $\beta \approx 2$. This behavior and the T dependence of $\Delta C_{\text{el}}(T)$ in the superconducting state are well described by two-band Eliashberg-theory for d -wave superconductors with weak pair-breaking due to nonmagnetic impurities.

This work was supported by the DFG through the SPP 1458, the E.-Noether program (WU 595/3-1 (S.W.)), and the EU-Japan project (No. 283204 SUPER-IRON). S.W. thanks the BMBF for support in the frame of the ERA.Net RUS project FeSuCo No. 245. We acknowledge fruitful discussion with K. Iida, A. Chubukov, S. Johnston, O. Dolgov, D. Evtushinsky as well as P.C. Canfield J. Zaanen, and P. Walmsley for stimulating interest. We thank also P. Chekhonin, and E. Ahrens for support in the experimental performance and valuable discussions.

SUPPLEMENTARY MATERIAL

In the present supplementary part we present our unpublished data for the specific heat of $\text{LaFeAsO}_{0.9}\text{F}_{0.1}$ employed in Fig. 3a for the BNC-scaling shown in the main text. We also provide additional data for the electrical resistivity of $\text{K}_{1-x}\text{Na}_x\text{Fe}_2\text{As}_2$ used there in the inset of Fig.3b. Furthermore, we give a detailed analysis of the magnetic impurity contribution in our samples and present the fitting parameters of the normal state SH. Finally, we provide x-ray data for the investigated single crystals.

The specific-heat of $\text{LaFeAsO}_{0.9}\text{F}_{0.1}$

Here, we present our unpublished $\text{LaFeAsO}_{0.9}\text{F}_{0.1}$ data with the aim to demonstrate that the La-1111 superconductors join also the cubic BNC-scaling. Polycrystalline $\text{LaFeAsO}_{0.9}\text{F}_{0.1}$ samples were prepared from pure components using a two-step solid-state reaction method [49]. Structural data and other physical properties of these samples are given in Refs. 48, 50. In Fig. S1 we show the specific heat C data for $\text{LaFeAsO}_{0.9}\text{F}_{0.1}$ in zero magnetic field (ZF) and applied magnetic fields of $H = 90$ kOe. To get an electronic contribution ΔC_{el} in the superconducting state we considered the difference $\Delta C_{\text{el}} = C(0) - C(9\text{T})$. This procedure provides ΔC_{el} in the range of 3 K below T_c taking into account that $dH_{c2}/T_c \approx 2.85$ T/K [48]. As shown in Fig. S1 this temperature range is sufficient to obtain the electronic specific heat jump ΔC_{el} for this compound.

Resistivity data of our $\text{K}_{1-x}\text{Na}_x\text{Fe}_2\text{As}_2$ samples

The resistivity data of $\text{K}_{1-x}\text{Na}_x\text{Fe}_2\text{As}_2$ single crystals for various x are shown in Fig. S2. In order to determine the clean limit value of T_{c0} we plot the T_c values of the investigated samples versus the experimental values of the residual resistivity ρ_0 as shown in the inset of Fig. 3b (main text). We note that $\text{K}_{1-x}\text{Na}_x\text{Fe}_2\text{As}_2$ is a multiband system. However, T_c is defined mainly by the strong superconducting band. Therefore, for the sake of simplicity, to estimate T_{c0} we fitted the experimental data by the single-band Abrikosov-Gor'kov (AG) formula modified for the d -wave case [51, 52]

$$-\ln\left(\frac{T_c}{T_{c0}}\right) = \psi\left(\frac{1}{2} + \frac{\alpha T_{c0}}{2\pi T_c}\right) - \psi\left(\frac{1}{2}\right), \quad (\text{S1})$$

where $\alpha = 1/[2\tau_{\text{eff}}T_{c0}]$ is the strong-coupling pair-breaking parameter and $\Gamma_{\text{eff}} = 1/\tau_{\text{eff}} \propto \rho_0$ is the an effective scattering rate due to impurities (created by the Na substitution). Then the clean limit value $T_{c0} = 3.5(1)$ K was obtained according to the analysis of the T_c suppression using τ_{eff} as an additional fitting parameter.

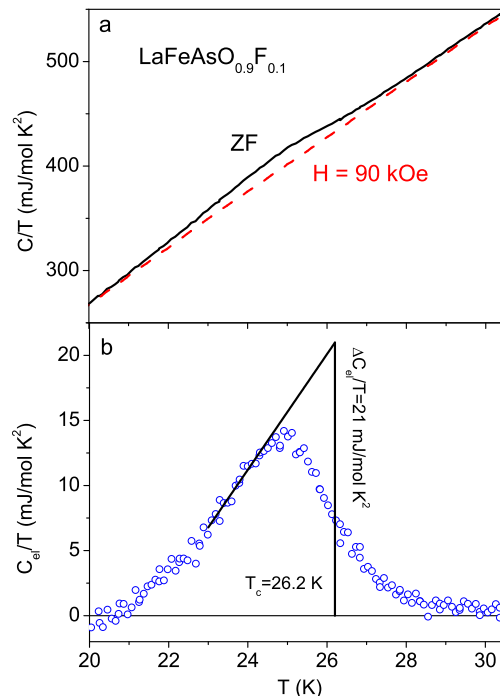


FIG. S1: (a) Temperature dependence of the specific heat of $\text{LaFeAsO}_{0.9}\text{F}_{0.1}$ in zero magnetic field (ZF) and applied magnetic fields $H = 90$ Oe. (b) Temperature dependence of the electronic specific heat $\Delta C_{\text{el}}/T = [C(0) - C(9\text{T})]/T$ near T_c .

It is seen in Fig. S2a that below 10 K the temperature dependence of resistivity deviates from the standard $\rho(T) = \rho_0 + AT^2$ Fermi-liquid behavior. This deviation is stronger for crystals with higher ρ_0 values. We note that this deviation does not necessarily mean that our samples are in a non-Fermi liquid regime. In particular, a subquadratic dependence can be expected in the case of multiband metals even when all the i bands follow the standard law $\rho_i(T) = \rho_{i0} + A_i T^2$. In this case the fit by the multiband equation $\rho(T) = 1/\sum_i(1/\rho_i(T))$ ($i=4$) provides a good description of the data as shown in Fig. S2a. However, one should assume that the scattering rates and the Fermi velocities are strongly band dependent.

Analysis of the magnetic impurity contribution

The magnetization data given in the inset of Fig. 1b of the main text can be fitted using two contributions: $m(H, T) = m_{\text{int}}(H, T) + m_{\text{imp}}(H, T)$, where m_{int} is the intrinsic magnetization and m_{imp} is the magnetic contribution of the impurity. We assume that $m_{\text{int}}(H, T) \approx \chi_s(T)H$ is dominated by the static spin susceptibility χ_s and other contributions are negligible [48]. To estimate the concentration of the magnetic impurities n in

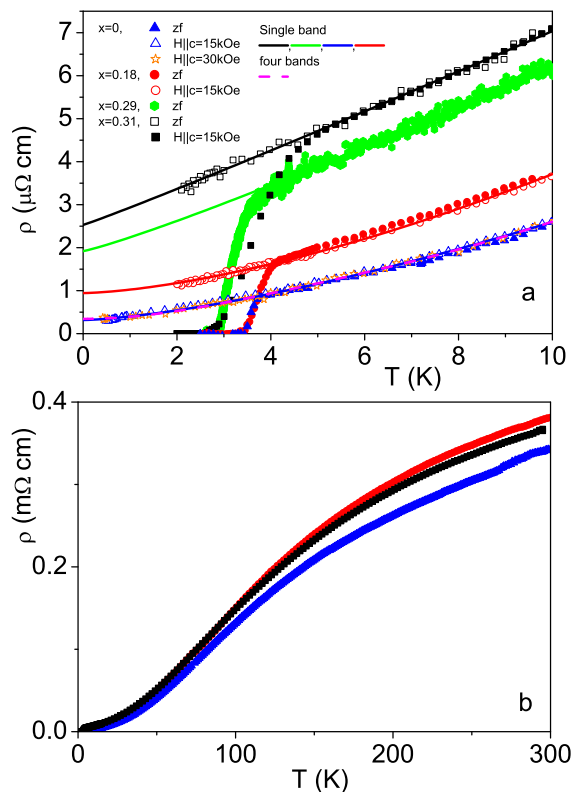


FIG. S2: Temperature dependence of the resistivity (a): below 10 K (the data for $x = 0.29$ are taken from Ref. 12), (b): zero field data up to 300K.

the samples we assumed that the impurity contribution is related to paramagnetic Fe^{+3} with $J=5/2$. In this case $m_{imp} = nJgB(H/T)$, where $B(H/T)$ is the Brillouin function, and g is the Landé factor. From the fit of the experimental data shown in the inset of Fig. 1b in the main text, we estimated that $n \lesssim 0.1\text{mol}\%$ for all investigated samples.

The main parameters for the normal state SH

The fitting parameters obtained from the fit of the normal-state specific heat data by $C(T) = \gamma_n T + \beta T^3 + \eta T^5$ shown in Fig. 2a in the main text are:

$$\text{For } x=0: \gamma_n = 99(2) \text{ mJ/mol K}^2, \beta = 0.51(5) \text{ mJ/molK}^4, \eta = 1.2(2) \cdot 10^{-3} \text{ mJ/molK}^6;$$

$$x = 0.19: \gamma_n = 98(3) \text{ mJ/mol K}^2, \beta = 0.51(5) \text{ mJ/molK}^4, \eta = 0.9(2) \cdot 10^{-3} \text{ mJ/molK}^6;$$

$$x = 0.29: \gamma_n = 99(2) \text{ mJ/mol K}^2, \beta = 0.51(4) \text{ mJ/molK}^4, \eta = 0.9(2) \cdot 10^{-3} \text{ mJ/molK}^6;$$

$$x = 0.31: \gamma_n = 98(6) \text{ mJ/mol K}^2, \beta = 0.52(5) \text{ mJ/molK}^4, \eta = 1.4(4) \cdot 10^{-3} \text{ mJ/molK}^6.$$

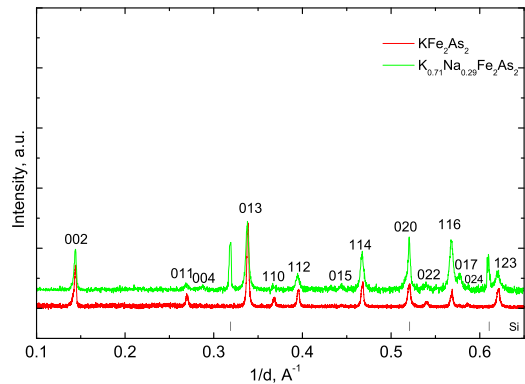


FIG. S3: The powder x-ray diffraction patterns for the stoichiometric KFe_2As_2 and Na doped samples.

x-ray analysis

To demonstrate the phase purity of the $\text{K}_{1-x}\text{Na}_x\text{Fe}_2\text{As}_2$ samples we performed powder x-ray diffraction measurements. The powders were obtained by milling the single crystals in an Ar atmosphere. The data for $x = 0$ and $x = 0.29$ are shown in Fig. S3. (In the latter case Si has been used as an internal standard.) It is seen that only reflections for the 122 phase are present in the data.

* Electronic address: v.grinenko@ifw-dresden.de

† Electronic address: s.l.drechsler@ifw-dresden.de

- [1] S.L. Bud'ko, Ni Ni, and P.C. Canfield, Phys. Rev. B **79**, 220516R (2009).
- [2] V.G. Kogan, Phys. Rev. B **81**, 184528 (2010).
- [3] C. Chaparro, L. Fang, H. Claus, A. Rydh, G.W. Crabtree, V. Stanev, W.K. Kwok, and U. Welp, Phys. Rev. B **85**, 184525 (2012).
- [4] V.G. Kogan, Phys. Rev. B **80**, 214532 (2009).
- [5] J. Zaanen, Phys. Rev. B **80**, 212502 (2009).
- [6] D. Kuzmanovski, A. Levchenko, M. Khodas, and M.G. Vavilov, arXiv:1401.1118v1 (2014).
- [7] M.G. Vavilov and A.V. Chubukov, Phys. Rev. B **84**, 214521 (2011).
- [8] M.G. Vavilov, A.V. Chubukov, and A.B. Vorontsov, Phys. Rev. B **84**, 140502(R) (2011).
- [9] J.-H. She, B.J. Overbosch, Y.-W. Sun, Y. Liu, K.E. Schalm, J.A. Mydosh, and J. Zaanen Phys. Rev. B **84**, 144527 (2011).
- [10] S.L. Bud'ko, M. Sturza, D.Y. Chung, M.G. Kanatzidis, and P. C. Canfield, Phys. Rev. B **87**, 100509(R) (2013).
- [11] J.-Ph. Reid, M.A. Tanatar, A. Juneau-Fecteau, R.T. Gordon, S.R. de Cotret, N. Doiron-Leyraud, T. Saito, H. Fukazawa, Y. Kohori, K. Kihou, C.H. Lee, A. Iyo, H. Eisaki, R. Prozorov, and L. Taillefer, Phys. Rev. Lett. **109**, 087001 (2012).
- [12] M. Abdel-Hafez, V. Grinenko, S. Aswartham, I. Morozov, M. Roslova, O. Vakaliuk, S. Johnston, D.V. Efremov,

- mov, J. van den Brink, H. Rosner, M. Kumar, C. Hess, S. Wurmehl, A.U.B. Wolter, B. Büchner, E.L. Green, J. Wosnitzer, P. Vogt, A. Reifemberger, C. Enss, M. Hempel, R. Klingeler, and S.-L. Drechsler, *Phys. Rev. B* **87**, 180507(R) (2013).
- [13] K. Hashimoto, A. Serafin, S. Tonegawa, R. Katsumata, R. Okazaki, T. Saito, H. Fukazawa, Y. Kohori, K. Kihou, C.H. Lee, A. Iyo, H. Eisaki, H. Ikeda, Y. Matsuda, A. Carrington, and T. Shibauchi, *Phys. Rev. B* **82**, 014526 (2010).
- [14] K. Okazaki, Y. Ota, Y. Kotani, W. Malaeb, Y. Ishida, T. Shimojima, T. Kiss, S. Watanabe, C.-T. Chen, K. Kihou, C.H. Lee, A. Iyo, H. Eisaki, T. Saito, H. Fukazawa, Y. Kohori, K. Hashimoto, T. Shibauchi, Y. Matsuda, H. Ikeda, H. Miyahara, R. Arita, A. Chainani, S. Shin, *Science* **337**, 1314 (2012).
- [15] D. Watanabe, T. Yamashita, Y. Kawamoto, S. Kurata, Y. Mizukami, T. Ohta, S. Kasahara, M. Yamashita, T. Saito, H. Fukazawa, Y. Kohori, S. Ishida, K. Kihou, C.H. Lee, A. Iyo, H. Eisaki, A.B. Vorontsov, T. Shibauchi, Y. Matsuda, arXiv: 1307.3408v1 (2013).
- [16] F. Hardy, R. Eder, M. Jackson, D. Aoki, C. Paulsen, T. Wolf, P. Burger, A. Böhm, P. Schweiss, P. Adelmann, R.A. Fisher, and C. Meingasta, arXiv:1309.5654v1 (2013).
- [17] S. Maiti, M.M. Korshunov, and A.V. Chubukov, *Phys. Rev. B* **85**, 014511 (2012).
- [18] R. Thomale, C. Platt, W. Hanke, J. Hu, and B.A. Bernevig, *Phys. Rev. Lett.* **107**, 117001 (2011).
- [19] S. Maiti and A.V. Chubukov, *Phys. Rev. B* **87**, 144511 (2013).
- [20] Supplement. Link to be added by the Journal.
- [21] F. Hardy, A. E. Böhm, D. Aoki, P. Burger, T. Wolf, P. Schweiss, R. Heid, P. Adelmann, Y.X. Yao, G. Kotliar, J. Schmalian, and C. Meingast, *Phys. Rev. Lett.* **111**, 027002 (2013).
- [22] V. Grinenko, S.-L. Drechsler, M. Abdel-Hafiez, S. Aswartham, A.U.B. Wolter, S. Wurmehl, C. Hess, K. Nenkov, G. Fuchs, D.V. Efremov, B. Holzapfel, J. van den Brink, and B. Büchner, *Phys. Status Solidi B* **250**, 593 (2013).
- [23] J.S. Kim, E.G. Kim, G.R. Stewart, X.H. Chen, and X.F. Wang, *Phys. Rev. B* **83**, 172502 (2011).
- [24] H. Fukazawa, T. Saito, Y. Yamada, K. Kondo, M. Hirano, Y. Kohori, K. Kuga, A. Sakai, Y. Matsumoto, S. Nakatsuji, K. Kihou, A. Iyo, C.H. Lee, and H. Eisaki, *J. Phys. Soc. Jpn.* **80**, SA118 (2011).
- [25] M. Abdel-Hafiez, S. Aswartham, S. Wurmehl, V. Grinenko, C. Hess, S.-L. Drechsler, S. Johnston, A.U.B. Wolter, and B. Büchner, H. Rosner, L. Boeri, *Phys. Rev. B* **85**, 134533 (2012).
- [26] S.L. Bud'ko, Y. Liu, T.A. Lograsso, and P.C. Canfield, *Phys. Rev. B* **86**, 224514 (2012).
- [27] S. Kittaka, Y. Aoki, N. Kase, T. Sakakibara, T. Saito, H. Fukazawa, Y. Kohori, K. Kihou, C.-H. Lee, A. Iyo, H. Eisaki, K. Deguchi, N.K. Sato, Y. Tsutsumi, and K. Machida, *J. Phys. Soc. Jpn.* **83**, 013704 (2014).
- [28] J.S. Kim, L.Y. Xing, X.C. Wang, C.Q. Jin, and G.R. Stewart, *Phys. Rev. B* **87**, 054504 (2013).
- [29] J.S. Kim, G.R. Stewart, S. Kasahara, T. Shibauchi, T. Terashima, and Y. Matsuda, *J. Phys.: Condens. Matter* **23**, 222201 (2011).
- [30] P. Walmsley, C. Putzke, L. Malone, I. Guillamon, D. Vignolles, C. Proust, S. Badoux, A.I. Coldea, M.D. Watson, S. Kasahara, Y. Mizukami, T. Shibauchi, Y. Matsuda, and A. Carrington, *Phys. Rev. Lett.* **110**, 257002 (2013).
- [31] J.S. Kim, G.R. Stewart, L.Y. Xing, X.C. Wang, and C.Q. Jin, *J. Phys.: Condens. Matter* **24**, 475701 (2012).
- [32] U. Stockert, M. Abdel-Hafiez, D.V. Evtushinsky, V.B. Zabolotnyy, A.U.B. Wolter, S. Wurmehl, I. Morozov, R. Klingeler, S.V. Borisenko, and B. Büchner, *Phys. Rev. B* **83**, 224512 (2011).
- [33] I. Morozov, A. Boltalin, O. Volkova, A. Vasiliev, O. Kataeva, U. Stockert, M. Abdel-Hafiez, D. Bombor, A. Bachmann, L. Harnagea, M. Fuchs, H.-J. Grafe, G. Behr, R. Klingeler, S. Borisenko, C. Hess, S. Wurmehl, and B. Büchner, *Cryst. Growth Des.* **10**, 4428 (2010).
- [34] F. Rullier-Albenque, D. Colson, A. Forget, and H. Alloul, *Phys. Rev. Lett.* **109**, 187005 (2012).
- [35] For the sake of completeness we mention that this result is compatible with the mentioned above non-Fermi liquid theory for $D = 2$ proposed in Ref. 5 and the large mass anisotropy of the order of 25 to 56 derived from the slopes of the upper critical field at T_c for the in-plane and out-of-plane directions. Since the applicability of the former is rather unclear at the moment, we will not discuss this case here.
- [36] In contrast to Ref. 5 from the point of view of the Fermi liquid based retarded Eliashberg-theory, our SH jumps are affected by the weak "strong" coupling renormalization (i.e. $\lambda_d < 1$), multiband effects, and a dominant pair-breaking. Hence, in a very rigorous sense there is *no* simple (x independent) power-law. The obtained total exponent $\beta \approx 2$ should be understood as an effective approximative description with reasonable accuracy.
- [37] G.R. Stewart, *Rev. Mod. Phys.* **83**, 1589 (2011).
- [38] A.F. Wang, B.Y. Pan, X.G. Luo, F. Chen, Y.J. Yan, J.J. Ying, G.J. Ye, P. Cheng, X.C. Hong, S.Y. Li, and X.H. Chen, *Phys. Rev. B* **87**, 214509 (2013).
- [39] V. Barzykin and L.P. Gor'kov, *Phys. Rev. B* **76**, 014509 (2007).
- [40] D.V. Efremov, M.M. Korshunov, O.V. Dolgov, A.A. Golubov, and P.J. Hirschfeld *Phys. Rev. B* **84**, 180512 (2011).
- [41] In our previous works [12, 22] γ_T has been ascribed phenomenologically to the observed cluster glass behavior. However, as one can see from the magnetization data shown in Fig. 1b there is no indication for such a behavior. Thus, a glassy contribution to the thermodynamics can be excluded for the present samples.
- [42] P. Popovich, A.V. Boris, O.V. Dolgov, A.A. Golubov, D.L. Sun, C.T. Lin, R.K. Kremer, and B. Keimer, *Phys. Rev. Lett.* **105**, 027003 (2010).
- [43] G. Preosti, H. Kim, and P. Muzikar, *Phys. Rev. B* **50**, 1259 (1994).
- [44] S. Johnston, M. Abdel-Hafiez, L. Harnagea, V. Grinenko, D. Bombor, Y. Krupskaya, C. Hess, S. Wurmehl, A.U.B. Wolter, B. Buechner, H. Rosner, S.-L. Drechsler, arXiv:1311.3516 (2013).
- [45] S. Aswartham, M. Abdel-Hafiez, D. Bombor, M. Kumar, A.U.B. Wolter, C. Hess, D.V. Evtushinsky, V.B. Zabolotnyy, A.A. Kordyuk, T.K. Kim, S.V. Borisenko, G. Behr, B. Büchner, and S. Wurmehl, *Phys. Rev. B* **85**, 224520 (2012).
- [46] T. Kobayashi, S. Miyasaka, S. Tajima, T. Nakano, Y. Nozue, N. Chikumoto, H. Nakao, R. Kumai, and Y. Murakami, *Phys. Rev. B* **87**, 174520 (2013).
- [47] K. Gofryk, J.C. Lashley, F. Ronning, D.J. Safarik, F.

- Weickert, J.L. Smith, A. Leithe-Jasper, W. Schnelle, M. Nicklas, and H. Rosner, Phys. Rev. B **85**, 224504 (2012).
- [48] V. Grinenko, K. Kikoin, S.-L. Drechsler, G. Fuchs, K. Nenkov, S. Wurmehl, F. Hammerath, G. Lang, H.-J. Grafe, B. Holzapfel, J. van den Brink, B. Büchner, and L. Schultz, Phys. Rev. B **84**, 134516, (2011).
- [49] A. Kondrat *et al.*, Eur. Phys. J. B **70**, 461 (2009).
- [50] G. Fuchs *et al.*, New J. Phys. **11**, 075007 (2009).
- [51] R.J. Radtke *et al.*, Phys. Rev. B **48**, 653 (1993).
- [52] Strictly speaking, to the best of our knowledge, there is no quantitative and semi-analytical multiband pair-breaking theory or T_c -formula available. However, from the general behavior of multiband systems the following scenario is expected. In relatively wide region where a quasi-linear decrease of T_c is observed the experimental data can be reasonably well described by a single

effective pair-breaking parameter which contains somehow averaged contributions from all bands, i.e. this region is expected to be described in the standard AG fashion as done here. Deviations are expected in the lower- T_c region, where isolated weakly coupled bands would already quench. In the present case due to the always present interband interaction T_c vanishes for all subsystems at the same T_c . As a consequence the contributions from the weaker bands continue to decay more slowly. The observation of such peculiarities would be helpful to extract parameters of the weakly coupled bands. The presently available experimental data cover only the upper "high"- T_c region and the applicability of an effective AG-approach seems to be justified.